RMetS
Royal Meteorological Society

Notes and Correspondence
Reply to comments on 'The influence of rotational frontogenesis and its associated shearwise vertical motions on the development of an upper-level front'

Andrea A. Lang[a] and Jonathan E. Martin[b]*
[a]*Department of Atmospheric and Environmental Sciences, University at Albany, NY, USA*
[b]*Department of Atmospheric and Oceanic Sciences, University of Wisconsin-Madison, WI, USA*

*Correspondence to: J. E. Martin, Department of Atmospheric and Oceanic Sciences, University of Wisconsin-Madison, 1225 W. Dayton Street, Madison, WI 53706, USA. E-mail: jemarti1@wisc.edu

Schultz (2012) proposes that our previous arguments regarding the initiation of along-flow geostrophic cold air advection during the upper frontogenesis process are incomplete. The core of his criticism, and the motivation for his call to include additional diagnostic calculations, hinges upon the assertion that the vertical vorticity can rotate isentropes relative to isohypses. In this response we derive an expression for the rate of change of $\nabla\phi$ that demonstrates that vorticity rotates $\nabla\theta$ and $\nabla\phi$ equally, in accord with our original statement to that effect. The derived expression also provides motivation to propose a revision of our previous conceptual model, highlighting the role of deformation instead of vorticity in the differential rotation of $\nabla\theta$ relative to $\nabla\phi$ that can contribute to the initiation of along-flow geostrophic temperature advection. Finally, we present a four-year synoptic-climatology suggesting that upper frontogenesis over central North America is, in fact, biased toward environments characterized by northwesterly flow.

Key Words: upper frontogenesis; geostrophic temperature advection; vorticity

Received 9 March 2012; Revised 19 June 2012; Accepted 23 August 2012; Published online in Wiley Online Library 30 October 2012

Citation: Lang AA, Martin JE. 2013. Reply to comments on 'The influence of rotational frontogenesis and its associated shearwise vertical motions on the development of an upper-level front'. *Q. J. R. Meteorol. Soc.* **139**: 273–279. DOI:10.1002/qj.2042

1. Introduction

Employing a partitioned **Q** vector approach, Lang and Martin (2010, hereafter LM10) examined the role of rotational frontogenesis, and its associated vertical circulation, in the process of upper frontogenesis. Such a quasi-geostrophic (QG) diagnostic approach was employed in order to isolate the discrete vertical circulation associated with the rotation of $\nabla\theta$ by the geostrophic wind. The role of that vertical circulation in initiating geostrophic cold air advection along the flow is particularly at issue in Schultz (2012).

Lang and Martin (2010) entered an ongoing debate between two competing hypotheses regarding the initiation of geostrophic cold air advection in the upper frontogenesis process and attempted to devise a more complete explanation that borrowed from both. Rotunno *et al.* (1994, hereafter RSS94), using idealized baroclinic channel model simulations, examined the intensification of an upper-level front from a nearly equivalent barotropic initial state. They argued that variations of along-flow subsidence produced, via differential adiabatic warming, a cyclonic rotation of the isentropes relative to the isohypses, resulting in the establishment of geostrophic cold air advection (RSS94, pp. 3389–3390). Schultz and Doswell (1999, hereafter

SD99) and Schultz and Sanders (2002, hereafter SS02), on the other hand, concluded that the onset of geostrophic cold air advection arises from the cyclonic rotation of isentropes relative to isohypses forced by the vorticity term in the rotational frontogenesis function. This explanation, however, depends implicitly upon whether the isentropes are differentially rotated relative to the isohypses. Schultz and Doswell (1999) acknowledge that 'the height field, as well as the thermal field, will be altered by the relative vorticity', but they go on to assert that 'the rotation of the isohypses by the vorticity is a secondary effect' (p. 2543, footnote).

Nearly all the issues raised in Schultz (2012) regarding LM10 revolve around the assertion that vorticity can differentially rotate isotherms relative to isohypses – an assertion that underlies the interpretation of certain diagnostic calculations made by SD99 and SS02, the absence of which in LM10 occasioned the present exchange. Therefore, in order to address these issues, our response is organized in the following manner. In section 2 we derive an expression for $\frac{\mathrm{d}}{dt_g}\nabla\phi$. The result proves our original proposition that 'vorticity rotates every vector field equally, and therefore cannot promote the *differential* rotation of $\nabla\theta$ relative to $\nabla\phi$ required to initiate along-flow *geostrophic* cold air advection'(LM10, p. 240). The derived expression also motivates a revision of the conceptual model originally offered in LM10 that suggests the RSS94 emphasis on along-flow subsidence gradients and the SD99 emphasis on kinematic rotational frontogenesis are interconnected aspects of a single dynamical process (rotational frontogenesis) that plays a central role in the initiation of along-flow geostrophic cold air advection during upper-level frontogenesis. In section 3 we present the initial results from a four-year climatology of upper-level fronts over continental North America that demonstrate a substantially higher incidence of northwesterly flow upper frontogenesis than that suggested by the climatology presented in SD99.

2. Vorticity rotates every vector field equally

One of Schultz's criticisms of LM10 is that we do not calculate all three terms in the rotational frontogenesis equation and so leave readers unable to determine the relative magnitudes of the vorticity and deformation contributions to rotation compared with that made by the tilting term. This admonition would be appropriate were the missing diagnostics able to testify to a differential rotation of $\nabla\theta$ relative to $\nabla\phi$ that would encourage the development of along-flow geostrophic cold air advection. We made clear in LM10 that we did not believe this to be the case (at least with regard to the role of vorticity, p. 240) but we did not prove it. In this section of our response, we demonstrate that the vorticity is never able to make such a contribution, directly contradicting the central conclusions of SD99 and SS02. We then proceed to show that, under certain circumstances, the deformation *can* make such a contribution but that it is equally powerless to do so if the initial state is equivalent barotropic. We end the section by proposing a revision of the original LM10 conceptual model that centres on the geostrophic deformation instead of the geostrophic vorticity as the primary kinematic agent of rotational frontogenesis. We begin by reviewing the role of geostrophic vorticity and deformation in altering the direction of $\nabla\theta$.

2.1. *Rotation of* $\nabla\theta$

Keyser *et al.* (1988) defined the vector frontogenesis function as

$$\mathbf{F} = \frac{\mathrm{d}}{dt}\nabla\theta$$

and noted that the **Q** vector is the geostrophic equivalent of **F** and so is expressed as

$$\mathbf{Q} = \frac{\mathrm{d}}{dt_{\mathrm{g}}}\nabla\theta.$$

The along-isentrope component of **Q** ($\mathbf{Q}_s$), which describes the rate of change of direction of $\nabla\theta$ produced by the geostrophic flow, is given by

$$\mathbf{Q}_s = \frac{\mathbf{Q}\cdot(\hat{k}\times\nabla\theta)}{|\nabla\theta|}\left[\frac{\hat{k}\times\nabla\theta}{|\nabla\theta|}\right]$$

where $\hat{\mathbf{s}} = \frac{\hat{k}\times\nabla\theta}{|\nabla\theta|}$ is the unit vector in the along-isentrope direction. This expression can be recast in terms of the geostrophic stretching (E_1) and shearing (E_2) deformations along with the geostrophic vorticity ($\zeta_{\mathbf{g}}$) as

$$\mathbf{Q}_s = \left[\frac{E_1\left(\frac{\partial\theta}{\partial x}\frac{\partial\theta}{\partial y}\right)}{|\nabla\theta|^2} - \frac{E_2\left(\frac{\partial\theta^2}{\partial x} - \frac{\partial\theta^2}{\partial y}\right)}{2|\nabla\theta|^2} + \frac{\zeta_{\mathbf{g}}}{2}\right](\hat{\mathrm{k}}\times\nabla\theta).$$

Thus, it is possible to separate the contributions of geostrophic deformation and geostrophic vorticity to the rotation of $\nabla\theta$ as

$$\mathbf{Q}_{s_{DEF}} = \left[\frac{E_1\left(\frac{\partial\theta}{\partial x}\frac{\partial\theta}{\partial y}\right)}{|\nabla\theta|^2} - \frac{E_2\left(\frac{\partial\theta^2}{\partial x} - \frac{\partial\theta^2}{\partial y}\right)}{2|\nabla\theta|^2}\right](\hat{\mathrm{k}}\times\nabla\theta) \quad (1a)$$

and

$$\mathbf{Q}_{s_{\mathrm{VORT}}} = \left[\frac{\zeta_{\mathrm{g}}}{2}\right](\hat{\mathrm{k}}\times\nabla\theta), \quad (2a)$$

respectively*. Recalling that $\mathbf{Q}_s = \mathbf{Q}_s\mathbf{s}$, the magnitude ($Q_s$) of the rotation of $\nabla\theta$ contributed by geostrophic vorticity can be written as

$$Q_{s_{\mathrm{VORT}}} = |\nabla\theta|\frac{\zeta_{\mathrm{g}}}{2}.$$

Rotation of isentropes can be assessed by considering the rate of change of α_θ, the angle between the x axis and the along-isentrope direction, **s**. From Figure 1 it is clear that

$$\tan\alpha_\theta = -\frac{\partial\theta}{\partial x}\Big/\frac{\partial\theta}{\partial y}.$$

*As a consequence of this separability, it is also possible to partition the total shearwise QG omega (related to $-2\nabla\cdot\mathbf{Q}_s$) into discrete portions attributable to the geostrophic vorticity and deformation as shown by Martin (1999).

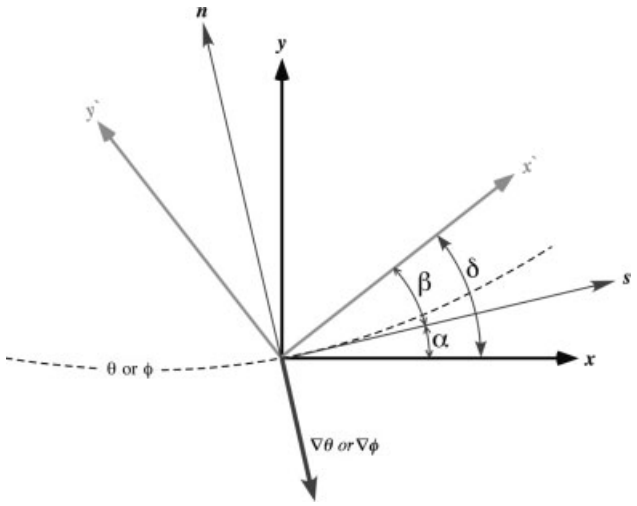

Figure 1. Schematic of the Cartesian systems (s, n) and (x',y') defined locally by rotating the original (x, y) system through the angles α and δ. The s axis is tangent to the isentropes (isohypses) with the n axis pointing toward lower θ (ϕ). The (x',y') system is defined such that the shearing deformation vanishes and x' serves as the axis of dilatation.

The Lagrangian derivative of that expression yields

$$\sec^2\alpha_\theta \frac{\mathrm{d}\alpha_\theta}{dt_\mathrm{g}} = \left(\frac{\mathrm{d}}{\mathrm{dt_g}}\left(\frac{\partial\theta}{\partial y}\right)\frac{\partial\theta}{\partial x} - \frac{\mathrm{d}}{\mathrm{dt_g}}\left(\frac{\partial\theta}{\partial x}\right)\frac{\partial\theta}{\partial y}\Big/\left(\frac{\partial\theta}{\partial y}\right)^2\right).$$

Keyser *et al.* (1988) showed that $Q_\mathrm{s} = -\frac{1}{|\nabla\theta|}\left(\frac{\mathrm{d}}{\mathrm{dt_g}}\left(\frac{\partial\theta}{\partial x}\right)\frac{\partial\theta}{\partial y} - \frac{\mathrm{d}}{\mathrm{dt_g}}\left(\frac{\partial\theta}{\partial y}\right)\frac{\partial\theta}{\partial x}\right)$ and, because $\cos\alpha_\theta = -\frac{\partial\theta}{\partial y}/|\nabla\theta|$, that $Q_s = |\nabla\theta|\frac{\mathrm{d}\alpha_\theta}{\mathrm{dt_g}}$. Given that the contributions to Q_s from geostrophic vorticity and deformation are separable, then

$$\left(\frac{\mathrm{d}\alpha_\theta}{\mathrm{dt_g}}\right)_\mathrm{VORT} = \frac{Q_{s\mathrm{VORT}}}{|\nabla\theta|} = \frac{\zeta_\mathrm{g}}{2}. \tag{3a}$$

By rotating coordinate axes such that the shearing deformation (E_2) is eliminated, $\mathbf{Q}_{sDEF}$ can be rewritten as

$$\mathbf{Q}_{\mathrm{s_{DEF}}} = \left[\frac{E\sin 2\beta_\theta}{2}\right](\hat{\mathrm{k}}\times\nabla\theta)$$

where E is the total deformation field and β_θ is the angle between the isentropes and the axis of dilatation of the total deformation field (Figure 1). This means that the magnitude of the rotation of $\nabla\theta$ made by the geostrophic deformation is given by

$$Q_{\mathrm{s_{DEF}}} = |\nabla\theta|\left[\frac{E\sin 2\beta_\theta}{2}\right]$$

and, because $Q_{\mathrm{s_{DEF}}} = |\nabla\theta|\left(\frac{d\alpha_\theta}{\mathrm{dt_g}}\right)_\mathrm{DEF}$, then /

$$\left(\frac{\mathrm{d}\alpha_\theta}{\mathrm{dt_g}}\right)_\mathrm{DEF} = \left[\frac{E\sin 2\beta_\theta}{2}\right]. \tag{4a}$$

2.2. *Rotation of* $\nabla\phi$

In order to quantify the differential rotation of $\nabla\theta$ relative to $\nabla\phi$ it is necessary to consider how the geostrophic flow can alter the direction of $\nabla\phi$. If we now define a vector $\mathbf{Y}$ as the rate of change, following the geostrophic flow, of the vector $\nabla\phi$, then $\mathbf{Y} = \frac{\mathrm{d}}{dt_\mathrm{g}}\nabla\phi = \frac{\partial}{\partial t}\nabla\phi + u_\mathrm{g}\frac{\partial}{\partial x}\nabla\phi + v_\mathrm{g}\frac{\partial}{\partial y}\nabla\phi$. Expanding this expression yields;

$$\begin{aligned}\mathbf{Y} = {} & \frac{\partial}{\partial x}\hat{i}\left(\frac{\partial\phi}{\partial t} + u_\mathrm{g}\frac{\partial\phi}{\partial x} + v_\mathrm{g}\frac{\partial\phi}{\partial y}\right)\\ & + \frac{\partial}{\partial y}\hat{j}\left(\frac{\partial\phi}{\partial t} + u_\mathrm{g}\frac{\partial\phi}{\partial x} + v_\mathrm{g}\frac{\partial\phi}{\partial y}\right) + \left(-\frac{\partial\mathbf{V}_\mathrm{g}}{\partial x}.\nabla\phi\right)\hat{i}\\ & + \left(-\frac{\partial\mathbf{V}_\mathrm{g}}{\partial y}.\nabla\phi\right)\hat{\mathrm{j}}.\end{aligned}$$

As the geostrophic wind cannot advect ϕ, this reduces to

$$\mathbf{Y} = \nabla\frac{\partial\phi}{\partial t} + \left(-\frac{\partial\mathbf{V}_\mathrm{g}}{\partial x}.\nabla\phi\right)\hat{i} + \left(-\frac{\partial\mathbf{V}_\mathrm{g}}{\partial y}.\nabla\phi\right)\hat{\mathrm{j}}.$$

$\mathbf{Y}$ can be split into components across- and along-isohypses that describe the changes in magnitude and direction of $\nabla\phi$, respectively. We can call the latter component $\mathbf{Y}_\mathrm{s}$ and it is equal to $\mathbf{Y}_\mathrm{s} = \frac{\mathbf{Y}\cdot(\hat{\mathrm{k}}\times\nabla\phi)}{|\nabla\phi|}\frac{(\hat{\mathrm{k}}\times\nabla\phi)}{|\nabla\phi|}$. As $f\mathbf{V}_\mathrm{g} = \hat{\mathrm{k}}\times\nabla\phi$,

$$\mathbf{Y}_\mathrm{s} = \left[\frac{f\mathbf{V}_\mathrm{g}\cdot\nabla\left(\frac{\partial\phi}{\partial t}\right) - fu_\mathrm{g}\left(\frac{\partial\mathbf{V}_\mathrm{g}}{\partial x}.\nabla\phi\right) - fv_\mathrm{g}\left(\frac{\partial\mathbf{V}_\mathrm{g}}{\partial y}.\nabla\phi\right)}{|\nabla\phi|^2}\right](\hat{\mathrm{k}}\times\nabla\phi).$$

Expressed in terms of the geostrophic stretching and shearing deformations and the geostrophic vorticity (and recalling that $fu_\mathrm{g} = -\frac{\partial\phi}{\partial y}$ and $fv_\mathrm{g} = \frac{\partial\theta}{\partial x}$, this can be rewritten as

$$\mathbf{Y}_\mathrm{s} = \left[\frac{f\mathbf{V}_\mathrm{g}\cdot\nabla\left(\frac{\partial\phi}{\partial t}\right)}{|\nabla\phi|^2} + \frac{E_1\left(\frac{\partial\phi}{\partial x}\frac{\partial\phi}{\partial y}\right)}{|\nabla\phi|^2} - \frac{E_2\left(\frac{\partial\phi^2}{\partial x} - \frac{\partial\phi^2}{\partial y}\right)}{2|\nabla\phi|^2} + \frac{\zeta_\mathrm{g}}{2}\right](\hat{\mathrm{k}}\times\nabla\phi)$$

making clear that the contributions to the rotation of $\nabla\phi$ by the geostrophic deformation and vorticity are separable as

$$\mathbf{Y}_{s\mathrm{DEF}} = \left[\frac{E_1\left(\frac{\partial\phi}{\partial x}\frac{\partial\phi}{\partial y}\right)}{|\nabla\phi|^2} - \frac{E_2\left(\frac{\partial\phi^2}{\partial x} - \frac{\partial\phi^2}{\partial y}\right)}{2|\nabla\phi|^2}\right](\hat{k}\times\nabla\phi) \tag{1b}$$

and

$$\mathbf{Y}_{s\mathrm{VORT}} = \frac{\zeta_\mathrm{g}}{2}(\hat{\mathrm{k}}\times\nabla\phi).$$

As $\mathbf{Y}_{s\mathrm{VORT}} = Y_{s\mathrm{VORT}}\mathbf{s}$, where $\mathbf{s} = \frac{\hat{\mathrm{k}}\times\nabla\phi}{|\nabla\phi|}$, we have $Y_{s\mathrm{vort}} = \frac{\zeta_\mathrm{g}}{2}|\nabla\phi|$. Defining the angle, α_ϕ, between the x axis and the along-isohypse direction, as $\alpha_\phi = \tan^{-1}\left(-\frac{\partial\phi/\partial x}{\partial\phi/\partial y}\right)$, a manipulation similar to that used to arrive at Eq. (3a) results in $Y_s = |\nabla\phi|\frac{d\alpha_\phi}{dt_\mathrm{g}}$. Therefore,

$$\left(\frac{d\alpha_\phi}{dt_\mathrm{g}}\right)_\mathrm{VORT} = \frac{\zeta_\mathrm{g}}{2} \tag{3b}$$

demonstrating that the geostrophic vorticity contributes identically to the rotation of $\nabla\phi$ and of $\nabla\theta$.

It should be noted that upon defining the Lagrangian derivative operator as $\frac{\mathrm{d}}{\mathrm{dt}} = \frac{\partial}{\partial t} + u\frac{\partial}{\partial x} + v\frac{\partial}{\partial y} + \omega\frac{\partial}{\partial p}$ as in SD99, the vector **Y** becomes

$$\mathbf{Y} = g\nabla w - \left(\frac{\partial \mathbf{V}}{\partial x}.\nabla\phi\right)\hat{i} - \left(\frac{\partial \mathbf{V}}{\partial y}.\nabla\phi\right)\hat{j} + \frac{\mathrm{RT}}{\mathrm{p}}\nabla\omega. \quad (5)$$

As the vorticity and deformation contributions reside in the middle two terms of Eq. (5), it can be shown (Appendix) that terms similar to Eqs (1b) and (2b) arise from use of the full wind, leading to the result that the vorticity of the full wind also rotates $\nabla\theta$ and $\nabla\phi$ equally. It follows that the vorticity cannot differentially rotate the isentropes relative to the isohypses and, therefore, cannot be responsible for initiating along-flow geostrophic temperature advection.

In light of this result, the calculations called for by Schultz (2012) to remedy a perceived shortcoming in LM10, calculations identical to those employed by SD99 and SS02, are not necessary to address the initiation of along-flow geostrophic cold air advection. Instead, the role of geostrophic deformation in rotating $\nabla\theta$ and $\nabla\phi$ should be considered.

As the rotation of $\nabla\phi$ by the geostrophic deformation (Eq. (1b)) has the same form as Eq. (1a), equivalent manipulations lead to the similar geometric form,

$$\mathbf{Y}_{s_{\mathbf{DEF}}} = \frac{E\sin 2\beta_\phi}{2}(\hat{\mathrm{k}} \times \nabla\phi)$$

where β_ϕ is the angle between the isohypses and the axis of dilatation of the total deformation field. Dividing by **s** yields $Y_{s_{\mathbf{DEF}}} = |\nabla\phi|\frac{E\sin 2\beta_\phi}{2} = |\nabla\phi|\left(\frac{d\alpha_\phi}{dt_\mathrm{g}}\right)_{\mathrm{DEF}}$. Therefore,

$$\left(\frac{d\alpha_\phi}{dt_\mathrm{g}}\right)_{\mathrm{DEF}} = \frac{E\sin 2\beta_\phi}{2}. \quad (4b)$$

Comparison of Eqs (4a) and (4b) reveals that if the flow is equivalent barotropic (i.e. θ and ϕ are everywhere parallel so that $\beta_\theta = \beta_\phi$), then the geostrophic† flow rotates $\nabla\theta$ and $\nabla\phi$ equally and cannot create regions of geostrophic temperature advection. In the case when these scalar fields are *not* parallel, the potential exists for geostrophic deformation (and *only* the deformation) to differentially rotate $\nabla\theta$ relative to $\nabla\phi$. A measure of this potential is

$$\left(\frac{d\alpha_\theta}{dt_\mathrm{g}}\right)_{\mathrm{DEF}} - \left(\frac{d\alpha_\phi}{dt_\mathrm{g}}\right)_{\mathrm{DEF}} = \frac{\mathrm{E}}{2}[\sin 2\beta_\theta - \sin 2\beta_\phi].$$

When this expression is positive (negative), $\nabla\theta$ is rotated cyclonically (anticyclonically) relative to $\nabla\phi$ and geostrophic cold (warm) air advection is encouraged. The Cartesian expression of this relationship, more amenable to direct calculation from modern gridded analyses, takes the form

$$\begin{aligned}&\left(\frac{d\alpha_\theta}{dt_\mathrm{g}}\right)_{\mathrm{DEF}} - \left(\frac{d\alpha_\phi}{dt_\mathrm{g}}\right)_{\mathrm{DEF}}\\ &= \frac{1}{|\nabla\theta|^2}\left[E_1\frac{\partial\theta}{\partial x}\frac{\partial\theta}{\partial y} - \frac{E_2}{2}\left(\frac{\partial\theta^2}{\partial x} - \frac{\partial\theta^2}{\partial y}\right)\right]\\ &- \frac{1}{|\nabla\phi|^2}\left[E_1\frac{\partial\phi}{\partial x}\frac{\partial\phi}{\partial y} - \frac{E_2}{2}\left(\frac{\partial\phi^2}{\partial x} - \frac{\partial\phi^2}{\partial y}\right)\right] \quad (6)\end{aligned}$$

†The results in (4a) and (4b) are also true for formulations using the full wind as is shown in the Appendix.

Thus, it is possible to calculate the differential rotation of $\nabla\theta$ relative to $\nabla\phi$ that is forced by the geostrophic deformation. We suggest that this measure, multiplied by $|\nabla\theta|$ (by analogy to Eqs (3a) and (4a)) defines what might be termed the *effective horizontal rotational frontogenesis* – that portion of the horizontal rotational frontogenesis that can actually modify the geostrophic temperature advection. A comparison of this effective horizontal rotational frontogenesis with the rotational frontogenesis associated with tilting $(-\frac{\partial\theta}{\partial p}\frac{\partial\omega_{\mathrm{QG}}}{\partial s})$ at a representative time from the case examined in LM10 is shown in Figure 2. It is clear that the effective horizontal rotational frontogenesis (Figure 2a) is much smaller than that afforded by tilting (Figure 2b), suggesting a predominant role for tilting in changing the geostrophic temperature advection.

Lang and Martin (2010) proposed a conceptual model, illustrated in their figure 13, which suggested that the development of along-flow geostrophic cold air advection was dependent on both kinematic rotation of $\nabla\theta$ and along-flow tilting. Given the re-evaluation of the kinematics offered in this response, it is likely that rotation by deformation provides the kinematic contribution that we mistakenly attributed to the vorticity in our original paper. We are currently undertaking the calculations necessary to re-examine the various contributions to this important process.

3. Comments on upper-level front climatologies

Schultz (2012) claims that observed climatologies of upper-level fronts do not support statements in LM10 regarding an 'observed preference' for the development of upper-level fronts in northwesterly flow. In support of his criticism, he cites a climatology of upper-level fronts presented in SD99 in which a preference for southwesterly flow is revealed. We believe that the SD99 climatology is biased toward identification of upper-level fronts in southwesterly flow by virtue of the manner in which it was constructed.

Schultz and Doswell (1999) used the National Meteorological Center (NMC) Daily Weather Map series for six winter seasons (December–February of 1988–89 through to 1993–94) to identify surface cyclones that crossed the west coast of North America between 35°N and 60°N. Once such surface cyclones were identified, the corresponding 500 hPa analyses were used to construct the climatology of the associated upper-level fronts. As illustrated by Roebber (1984, figure 10(b)), the region along the west coast of North America, from northern California to Alaska (approximately from 35°N to 60°N), is a characteristic region for dissipation of surface cyclones. Dissipating extratropical cyclones are typically occluded and characterized by southwesterly flow aloft. Analysis of cyclone tracks in the Gulf of Alaska region by Campa and Wernli (2012, figure 5(d)) also demonstrate the preference for West Coast landfalling cyclones to exhibit southwesterly flow aloft. As a result, basing a climatology of upper-level fronts on their association with landfalling cyclones along the west coast of North America introduces a notable bias toward upper-level fronts in southwesterly flow. We contend that a climatology so constructed is not likely to be representative of the variety of cases observed over North America and to suggest otherwise serves only to reinforce the original bias.

In order to address this concern, we have constructed a four-year climatology of North American upper-level fronts occurring in December–February of 2007–08 through to

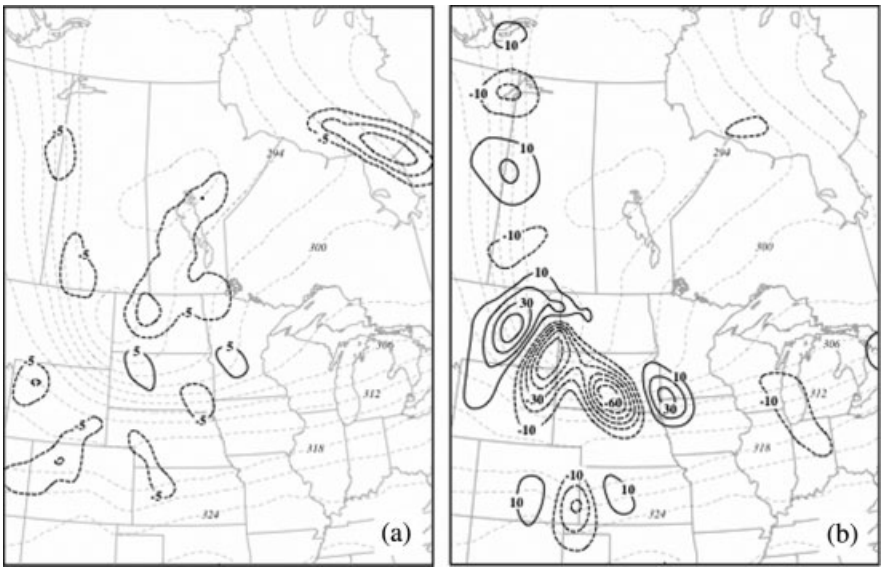

Figure 2. (a) Effective horizontal rotational frontogenesis (see text for explanation) and potential temperature at 400 hPa at 1200 UTC 12 November 2003. Bold solid (dashed) lines are effective horizontal rotational frontogenesis labelled in units of 10^{-10} K m^{-1}s^{-1} and contoured every 5 (-5) $\times$ 10^{-10} K m^{-1}s^{-1} beginning at 5 (-5) $\times$ 10^{-10} K m^{-1}s^{-1}. Potential temperature labelled in K and contoured every 3 K. (b) Tilting rotational frontogenesis and potential temperature at 400 hPa at 1200 UTC 12 November 2003. Tilting frontogenesis labeled as in (a) but contoured every 10 (-10) $\times$ 10^{-10} K m^{-1}s^{-1} beginning at 10 (-10) $\times$ 10^{-10} K m^{-1}s^{-1}. Potential temperature labeled and contoured as in (a).

2010–11. The analysis region was a box centred over North America, from 25°N to 60°N and 60°W to 130°W. Using the twice-daily (0000 UTC and 1200 UTC) National Centers for Environmental Prediction's (NCEP's) Global Forecast System (GFS) analyses (at 1° × 1° resolution), the value and location of the maximum magnitude of the potential temperature gradient ($|\nabla\theta|$) at 500 hPa within the box were recorded. The data were then sorted by the $|\nabla\theta|$, keeping only the 483 instances in which the $|\nabla\theta| > 6$ K (100 km)$^{-1}$. Beginning with the case exhibiting the maximum $|\nabla\theta|$ (13.8 K (100 km)$^{-1}$ on 28 December 2008), subsequent instances that were not at least 60 h removed from a stronger case were eliminated from the data set. This filtering resulted in 104 unique cases, or roughly 24–28 cases per winter. These cases were then placed into one of eight wind-direction bins based on wind direction at the location of the maximum 500 hPa $|\nabla\theta|$[‡].

Table 1 contains the results of this North American climatology of upper-level fronts. The analysis reveals notably different results than those presented in the SD99 climatology. Of the 104 upper-level front cases examined here only 25% (26 cases) occurred in southwesterly flow, compared with 44% in the SD99 climatology. Likewise, more upper front cases were present in northwesterly flow, 30.7% (32 cases), compared with only 14% in the SD99 analysis. When expanded to all cases with a northerly component to the wind, this group made up 39.6% (42 cases) of the North American climatology. In addition, the northwesterly (southwesterly) flow North American upper-level fronts tended to form in the western (eastern) half of the continent.

These results are further illustrated by considering event-centred composites of the four most common wind-direction groups shown in Figure 3. These composites are based upon the synoptic times of greatest intensity for the 104 unique events identified in the climatology. Note the clear eastward progression of event-types across North America with northerly flow events (Figure 3a) farthest west and southwesterly flow events (Figure 3d) farthest east. We are currently constructing composites from all 483 instances of strong upper tropospheric fronts in order to identify additional aspects of the life cycle of these features.

The results from this new climatology offer compelling evidence that the LM10 case is indeed representative for its location and that there is an 'observed preference' for northwesterly flow upper level fronts in western North America. These preliminary results make clear that the SD99 climatology has limited applicability to cases that occur over North America. The discrepancies between the two climatologies are being further considered in current research on this subject.

Appendix

Keyser *et al.* (1988) showed that the rotational frontogenesis vector is given by

$$\mathbf{F}_s = F_s\mathbf{s} = \frac{|\nabla\theta|}{2}[\zeta + E\sin 2\beta_\theta]\left(\frac{\hat{\mathrm{k}}\times\nabla\theta}{|\nabla\theta|}\right).$$

They further showed that $F_s = |\nabla\theta|\frac{d\alpha_\theta}{\mathrm{dt}}$ where α_θ is the angle between the x-axis and the isentropes. Schultz and Doswell (1999) expanded this expression by defining the Lagrangian operator as $\frac{\mathrm{d}}{\mathrm{dt}} = \frac{\partial}{\partial t} + u\frac{\partial}{\partial x} + v\frac{\partial}{\partial y} + \omega\frac{\partial}{\partial p}$. Their expression for F_s is given by

$$F_s = \frac{|\nabla\theta|}{2}[\zeta + E\sin 2\beta_\theta] + \frac{1}{|\nabla\theta|}\left(\frac{\partial\theta}{\partial p}\right)[\hat{\mathrm{k}}\cdot(\nabla_\mathrm{h}\omega\times\nabla_\mathrm{h}\theta)]$$

demonstrating that contributions to rotation of $\nabla\theta$ made by vorticity and deformation are not changed by expansion to the third dimension. Thus, employing the full wind,

[‡]There were no members in the Southerly, Easterly, or Southeasterly flow categories.

Table 1. Statistics of North American upper-level front cases, December to February 2007–08 to 2010–11.

Wind direction	Northeasterly	Northerly	Northwesterly	Westerly	Southwesterly
Wind direction range	22.5° – 67.4°	337.5° – 360° or 0° – 22.4°	292.5° – 337.4°	247.5° – 292.4°	202.5° – 247.4°
Number in bin	2	8	32	36	26
Percentage of total	1.6	7.7	30.7	34.6	25.0
Centre latitude	NA	40.25° N	40.66° N	35.75° N	38.35° N
Centre longitude	NA	117.13° W	105.66° W	90.33° W	88.69° W

NA, not applicable.

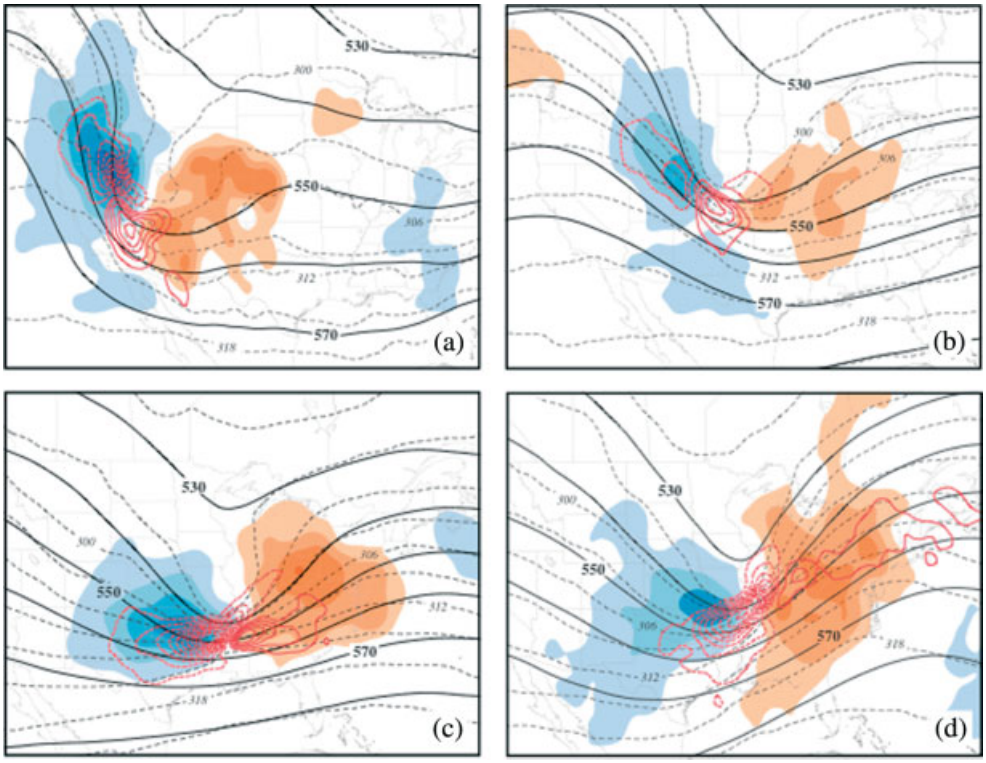

Figure 3. Composite analysis of December, January and February upper tropospheric fronts from the cases used in the four winter (2007–08 through to 2010–11) climatology presented in Table 1. The cases are binned by prevailing upper level flow direction with (a) northerly flow cases, (b) northwesterly flow cases, (c) westerly flow cases and (d) southwesterly flow cases. For all composites, the 500 hPa geopotential height is contoured (thick) every 100 m, θ is contoured (dashed) every 3 K, geostrophic temperature advection is contoured in red solid (dashed) every $3(-3) \times 10^{-4}$ K s^{-1} beginning at $1(-1) \times 10^{-4}$ K s^{-1}, and ω is shaded every 1 bar s^{-1} with ascent (descent) in orange (blue).

the separable contributions to $\frac{d\alpha_\theta}{\mathrm{dt}}$ made by vorticity and deformation are $\left(\frac{\mathrm{d}\alpha_\theta}{dt}\right)_{VORT} = \frac{\zeta}{2}$ and

$$\left(\frac{d\alpha_\theta}{\mathrm{dt}}\right)_{\mathrm{DEF}} = \frac{E \sin 2\beta_\theta}{2}. \tag{A1}$$

Upon defining the Lagrangian derivative operator as $\frac{\mathrm{d}}{\mathrm{dt}} = \frac{\partial}{\partial t} + u\frac{\partial}{\partial x} + v\frac{\partial}{\partial y} + \omega\frac{\partial}{\partial p}$, the vector $\mathbf{Y}$ becomes

$$\mathbf{Y} = g\nabla w - \left(\frac{\partial \mathbf{V}}{\partial x} \cdot \nabla\phi\right)\hat{i} - \left(\frac{\partial \mathbf{V}}{\partial y} \cdot \nabla\phi\right)\hat{j} + \frac{RT}{p}\nabla\omega. \tag{A2}$$

The rate of change of the direction of $\nabla\phi$ following the flow is given by

$$\mathbf{Y}_\mathrm{s} = \frac{\mathbf{Y} \cdot (\hat{\mathrm{k}} \times \nabla\phi)}{|\nabla\phi|} \frac{(\hat{\mathrm{k}} \times \nabla\phi)}{|\nabla\phi|}. \tag{A3}$$

As only the middle two terms of Eq. (A2) contain derivatives of the horizontal wind, the contributions of vorticity and deformation to rotation of $\nabla\phi$ reside within the sum of those terms. Thus,

$$\mathbf{Y}_{\mathrm{s_{DEF+VORT}}} = \left[\left(-\frac{\partial \mathbf{V}}{\partial x} \cdot \nabla\phi\right)\left(-\frac{\partial\phi}{\partial y}\right) + \left(-\frac{\partial \mathbf{V}}{\partial y} \cdot \nabla\phi\right)\left(\frac{\partial\phi}{\partial x}\right)\right] \left(\frac{\hat{\mathrm{k}} \times \nabla\phi}{|\nabla\phi|^2}\right) \tag{A4}$$

which can be rewritten as

$$\mathbf{Y}_{\mathrm{s_{DEF+VORT}}} = \left[\frac{E_1 \frac{\partial\phi}{\partial x}\frac{\partial\phi}{\partial y}}{|\nabla\phi|} - \frac{E_2\left(\frac{\partial\phi^2}{\partial x} - \frac{\partial\phi^2}{\partial y}\right)}{2|\nabla\phi|} + \frac{|\nabla\phi|\zeta}{2}\right] \left(\frac{\hat{\mathrm{k}} \times \nabla\phi}{|\nabla\phi|}\right) \tag{A5}$$

or

$$\mathbf{Y}_{\mathrm{s_{DEF+VORT}}} = \frac{|\nabla\theta|}{2}[\zeta + E \sin 2\beta_\phi] \left(\frac{\hat{\mathrm{k}} \times \nabla\phi}{|\nabla\theta|}\right) \tag{A6}$$

Thus, the magnitudes of the rotation forced by the vorticity and the deformation are $Y_{s_{VORT}} = \frac{|\nabla\theta|}{2}(\zeta)$ and $Y_{s_{DEF}} = \frac{|\nabla\theta|}{2}(E \sin 2\beta_\phi)$. As shown previously, with reference to Figure 1, because $\alpha_\phi = \tan^{-1}\left(-\frac{\partial\phi}{\partial x}/\frac{\partial\phi}{\partial y}\right)$, then $Y_s = |\nabla\theta|\frac{d\alpha_\phi}{dt}$.

Therefore,

$$\left(\frac{d\alpha_\phi}{dt}\right)_{VORT} = \frac{\zeta}{2} \text{ and } \left(\frac{d\alpha_\phi}{dt}\right)_{DEF} = \frac{E \sin 2\beta_\phi}{2}.$$

References

Campa J, Wernli H. 2012. A PV perspective on the vertical structure of mature midlatitude cyclones in the northern hemisphere. *J. Atmos. Sci.* **69**: 725–740.

Keyser D, Reeder MJ, Reed RJ. 1988. A generalization of Petterssen's frontogenesis function and its relation to the forcing of vertical motion. *Mon. Weather Rev.* **116**: 762–780.

Lang AA, Martin JE. 2010. The influence of rotational frontogenesis and its associated shearwise vertical motion on the development of an upper-level front. *Q. J. R. Meteorol. Soc.* **136**: 239–252.

Martin JE. 1999. The separate roles of geostrophic vorticity and deformation in the midlatitude occlusion process. *Mon. Weather Rev.* **127**: 2404–2418.

Roebber P. 1984. A statistical analysis and updated climatology of explosive cyclones. *Mon. Weather Rev.* **112**: 1577–1589.

Rotunno R, Skamarock WC, Snyder C. 1994. An analysis of frontogenesis in numerical simulations of baroclinic waves. *J. Atmos. Sci.* **51**: 3373–3398.

Schultz DM. 2012. Comment on 'The influence of rotational frontogenesis and its associated shearwise vertical motion on the development of an upper-level front' by A. A. Lang and J. E. Martin (January 2010, **136**: 239–252). *Q. J. R. Meteorol. Soc.*, DOI: 10.1002/qj.1871.

Schultz DM, Doswell III CA. 1999. Conceptual models of upper-level frontogenesis in southwesterly and northwesterly flow. *Q. J. R. Meteorol. Soc.* **125**: 2535–2562.

Schultz DM, Sanders F. 2002. Upper-level frontogenesis associated with the birth of mobile troughs in northwesterly flow. *Mon. Weather Rev.* **130**: 2593–2610.

